



Title	Molecular Basis for Herpesvirus Entry Mediator Recognition by the Human Immune Inhibitory Receptor CD160 and Its Relationship to the Cosignaling Molecules BTLA and LIGHT
Author(s)	Kojima, Rieko; Kajikawa, Mizuho; Shiroishi, Mitsunori; Kuroki, Kimiko; Maenaka, Katsumi
Citation	Journal of Molecular Biology, 413(4), 762-772 <a href="https://doi.org/10.1016/j.jmb.2011.09.018">https://doi.org/10.1016/j.jmb.2011.09.018</a>
Issue Date	2011-11-04
Doc URL	<a href="http://hdl.handle.net/2115/47962">http://hdl.handle.net/2115/47962</a>
Type	article (author version)
Additional Information	There are other files related to this item in HUSCAP. Check the above URL.
File Information	JMB413-4_762-772.pdf



[Instructions for use](#)

**Molecular basis for herpesvirus entry mediator recognition by the human immune inhibitory receptor CD160 and its relationship to the cosignaling molecules BTLA and LIGHT**

**Rieko Kojima<sup>1,2</sup>, Mizuho Kajikawa<sup>2</sup>, Mitsunori Shiroishi<sup>2</sup>,**

**Kimiko Kuroki<sup>1,2</sup>, and Katsumi Maenaka<sup>1,2,3,\*</sup>**

<sup>1</sup>Laboratory of Biomolecular Science, Faculty of Pharmaceutical Sciences, Hokkaido University, Kita-12, Nishi-6, Kita-ku, Sapporo 060-0812, Japan; <sup>2</sup>Medical Institute of Bioregulation, Kyushu University, 3-1-1 Maidashi, Higashi-ku, Fukuoka 812-8582, Japan; <sup>3</sup>CREST, Japan Science and Technology Agency, Saitama 332-0012, Japan.

\*Correspondence: Katsumi Maenaka, Laboratory of Biomolecular Science, Faculty of Pharmaceutical Sciences, Hokkaido University, Kita-12, Nishi-6, Kita-ku, Sapporo 060-0812, Japan; E-mail: maenaka@pharm.hokudai.ac.jp

## **ABSTRACT**

CD160 was recently identified as a T cell coinhibitory molecule that interacts with the herpesvirus entry mediator (HVEM) on antigen-presenting cells to deliver a potent inhibitory signal to CD4<sup>+</sup> T cells. HVEM also binds to the coinhibitory receptor BTLA (B- and T-lymphocyte attenuator) and the costimulatory receptor LIGHT (which is homologous to lymphotoxins, exhibits inducible expression, and competes with the herpes simplex virus glycoprotein D for HVEM, a receptor expressed by T lymphocytes, or TNFSF14), thus regulating the CD160/BTLA/LIGHT/HVEM signaling pathway. To date, the detailed properties of the formation of these complexes, especially HVEM binding to the newly identified receptor CD160, and the relationship of CD160 with BTLA and LIGHT are still unclear. We performed N-terminal sequencing and a mass spectrometric analysis, which revealed that the extracellular domain of CD160 exists primarily in the monomeric form. The surface plasmon resonance (SPR) analysis revealed that CD160 binds directly to the cysteine-rich domain (CRD) 1-3 of HVEM with a similar affinity to, but slower dissociation rate than, that of BTLA. Notably, CD160 competed with BTLA for binding to HVEM, in contrast, LIGHT did not affect HVEM binding to either CD160 or BTLA. The results of a mutagenesis study of HVEM also suggest that the CD160 binding region on HVEM was slightly different than, but overlapped with, the BTLA binding site. Interestingly, an anti-CD160 antibody exhibiting antiangiogenic properties blocked CD160-HVEM binding. These results provide insight into the molecular architecture of the CD160/BTLA/LIGHT/HVEM signaling complex that regulates immune function.

Key words: CD160, HVEM, cosignaling molecules, T cell regulation

## INTRODUCTION

T cell activation requires two signals: the T cell receptor (TCR) recognition of the major histocompatibility complex (MHC)/peptide complex and the cosignal delivered by the interaction between the cosignaling molecule and its receptor<sup>1;2</sup>. The cosignaling molecules function as costimulatory or coinhibitory molecules because of their functional effect upon host immune responses. TCR engagement without costimulation leads to suboptimal T cell activation and unresponsiveness to the antigen during secondary stimulation, a phenomenon called T cell anergy<sup>3</sup>. Cosignaling molecules control T cell activation by regulating T cell proliferation, cytokine production, cytotoxicity, T cell apoptosis, and survival<sup>4;5</sup>.

CD160 (murine CD160 is named BY55) was recently identified as a coinhibitory molecule that binds to one of the TNF receptor superfamily members, herpesvirus entry mediator (HVEM) (also called HveA or TNFRSF14), which is expressed on the surface of a broad range of immune cells, including T cells, B cells, natural killer (NK) cells, and dendritic cells, as well as endothelial cells<sup>6</sup>. CD160 is a type-I membrane protein with one immunoglobulin (Ig)-V set domain in its extracellular region, and it is expressed on NK cells, NKT cells, intraepithelial T cells,  $\gamma\delta$ TCR<sup>+</sup> T cells, CD8<sup>+</sup> T cells, and CD4<sup>+</sup> T cells<sup>6</sup>. Cai et al. recently demonstrated that the CD160-HVEM interaction inhibits CD4<sup>+</sup> T cell activation<sup>7</sup>. Moreover, several reports have indicated that CD160 has a significant stimulatory effect on immune responses, including NK and CD8<sup>+</sup> T cell effector functions<sup>8;9;10</sup>. A pathological study revealed that the expression level of CD160, as well as those of other immunosuppressive genes, increased in the lymphatic tissue of HIV-1-infected patients who were in the acute stage of the disease<sup>11</sup>. CD160 was also up-regulated in exhausted CD8<sup>+</sup> T cells in a mouse model of a chronic lymphocytic choriomeningitis virus (LCMV) infection<sup>12</sup>. These emerging details suggest that CD160 is one of the key cosignaling molecules controlling immune responses. Interestingly, CD160 is mainly

glycosylphosphatidylinositol (GPI)-anchored; thus, it is likely to be located in lipid rafts, as suggested by a cell surface staining study <sup>7</sup>. However, due to the lack of definitive signaling components, its signaling mechanism has not been clarified.

With regard to CD160 ligands, it is not yet fully understood whether CD160 can bind to MHC class I molecules (either a wide-range or a specific-allele (HLA-Cw3 or HLA-G1)) <sup>7; 8; 9; 10</sup>. A newly identified interaction between CD160 and HVEM has been confirmed by cellular-level function studies and binding studies, which also have demonstrated that the cysteine-rich domain (CRD) 1 of HVEM is essential for CD160 binding <sup>13</sup>. However, the underlying molecular properties mediating the precise binding of CD160 to HVEM and the relationship between CD160 and other HVEM receptors are still poorly understood.

Intriguingly, HVEM, the ligand of CD160, activates both stimulatory and inhibitory pathways and serves as a molecular switch by engaging at least five receptors: two costimulatory molecules, two coinhibitory molecules, and the herpes simplex virus (HSV) envelope glycoprotein D (gD). The costimulatory HVEM receptors consist of the TNF-related cytokine LIGHT (which is homologous to lymphotoxins, exhibits inducible expression, and competes with HSV gD for HVEM, a receptor expressed by T lymphocytes, or TNFSF14) and lymphotoxin- $\alpha$  (LT $\alpha$ ). LIGHT is a type-II membrane protein, and it forms a homotrimer on the cell surface in the same manner as other TNF family members. LIGHT is expressed on immature dendritic cells (DC), granulocytes, monocytes, and activated T cells <sup>6</sup>. LIGHT and HVEM are predicted to form a 3:3 complex, and their interaction delivers costimulatory signals that lead to T cell activation <sup>14; 15; 16; 17; 18</sup> and enhanced production of pro-inflammatory cytokines <sup>15; 19; 20; 21; 22</sup>. The coinhibitory molecules consist of CD160 and BTLA (the CD28 family member B- and T-lymphocyte attenuator). BTLA is a type-I membrane protein with an extracellular Ig-V domain, and it is broadly expressed on hematopoietic cells, including CD8+ T

cells, CD4<sup>+</sup> T cells, B cells, dendritic cells, macrophages, and NK cells. BTLA binds to CRD1 of HVEM to form a 1:1 complex<sup>23</sup>. BTLA-deficient mice exhibited hypersensitivity to TCR stimulation<sup>24; 25</sup> and persistent inflammation of the lung in an acute allergic airway inflammation model<sup>26</sup>. These data suggest that BTLA plays critical inhibitory roles in suppressing T cell activation. Alternatively, HVEM<sup>-/-</sup> mice exhibit overactivation of the T cell response<sup>22</sup>; thus, the essential, non-redundant function of HVEM is inhibitory. These results suggest that the coinhibitory HVEM receptors, CD160 and BTLA, play important roles in the regulation and maintenance of T cell immune responses.

Cai et al. demonstrated by confocal microscopy that GPI-anchored CD160 is present in discrete patches of the plasma membrane and does not colocalize with BTLA<sup>7</sup>. Furthermore, CD3 does colocalize with CD160, suggesting that CD160 is likely translocated into lipid rafts along with immune signaling complexes including TCR/CD3. These results introduced the possibility that CD160 may have discrete (and/or complementary) roles in the regulation of T cell function relative to those of BTLA. From another attractive viewpoint, the CD160/HVEM and BTLA/HVEM interactions are so far the only examples of signaling complexes between members of the Ig and TNFR superfamilies of immune cell surface receptors.

A recent study of HVEM binding to HSV gD, as well as to other HVEM receptors, showed that gD can block the binding of HVEM to BTLA but not to LT $\alpha$  and LIGHT<sup>13</sup>. Furthermore, BTLA did not interfere with HVEM binding to LT $\alpha$  and LIGHT<sup>13</sup>. With regard to CD160, the competition study for the HVEM binding of CD160 and BTLA was performed at the cellular level, but this did not yield a definitive result because the inhibition of BTLA-HVEM binding by excess CD160-Ig protein was not clearly observed<sup>7</sup>. The understanding of CD160-mediated regulation of the HVEM pathway of T cell function remains quite limited.

Here, we have elucidated the molecular characteristics of CD160 and the binding of CD160 to

HVEM using surface plasmon resonance (SPR) and competition binding studies for the other HVEM receptors, BTLA and LIGHT. First, we show that the extracellular domain of CD160 primarily exists in the monomeric form, as revealed by comprehensive techniques, including N-terminal amino acid sequence analysis and mass spectrometry. These data essentially preclude the possibility that CD160 can exist as a homotrimer, which is in contrast to the report by Anumanthan et al. <sup>27</sup>. We also demonstrate that the anti-CD160 antibody CL1-R2, which exhibited antiangiogenic activity in several animal models of neovascularization <sup>28</sup>, blocks CD160 binding to HVEM. CD160 directly interacts with HVEM with low affinity, which is consistent with a previous report <sup>13</sup>. Although this characteristic is similar to that of BTLA binding to HVEM, CD160 exhibits a slower dissociation rate than does BTLA, which might confer stronger signaling. Notably, CD160 competes with BTLA for HVEM binding, and a series of HVEM mutants that either decreased or completely lost the ability to bind to BTLA <sup>23</sup> also exhibited reduced CD160 binding, but to a different extent. Collectively, these results suggest that CD160 has various similar and distinct HVEM binding properties relative to those of BTLA and that these proteins can form a 3:3:3 (CD160 or BTLA : LIGHT : HVEM) full signaling complex. Finally, we discuss the implications for the function of CD160 in the immunoregulatory CD160/BTLA/HVEM pathway.

## RESULTS AND DISCUSSION

*CD160 exists in the monomeric form.*

One group previously reported that CD160 existed as a highly disulfide-linked homotrimer<sup>27</sup>; however, a recent study revealed that baculovirus-expressed CD160 existed in a monomeric form<sup>13</sup>. Thus, to clarify the precise molecular characteristics of CD160 under physiological conditions, the entire extracellular region of CD160 (residues 1-159) was expressed in human HEK293S GnTI<sup>-</sup> cells and designated CD160h. The CD160h protein was purified using Ni-NTA column chromatography followed by gel filtration chromatography (**Figure 1(A)**). A western blot analysis of the eluted fractions with an anti-6xHis antibody under non-reducing conditions (**Figure 1 (B)**) clearly indicated that CD160h predominantly existed in the monomeric form (fractions 4-6). The other fractions (1 to 3) in **Figure 1A**, which might include higher molecular weight forms, contained only a slight amount of the disulfide-linked CD160h dimer (**Figure 1 (B)**), and trimers or multimers were barely detectable. MALDI-TOF mass analyses of the main fractions also showed only the monomeric molecular mass of CD160 (**Supplemental Figure 1**). Furthermore, N-terminal amino acid sequence analyses of this fraction revealed that the CD160h extracellular region starts with the sequence  $_{27}\text{INITS}_{31}$  (**Figure 1 (C)**), which is consistent with the recently updated prediction by the “SignalP 3.0” program (<http://www.cbs.dtu.dk/services/Signal>; the previous version of this program calculated  $_{26}\text{CINIT}_{30}$  as the starting sequence). This analysis suggests that the extracellular domain of CD160 contains five cysteines after cleavage of the signal sequence (**Figure 1 (C), boxed**). A homology alignment demonstrated that CD160 should form two intramolecular disulfide bonds and have one free cysteine, which excludes the possibility of the formation of the previously reported intermolecularly disulfide-linked homotrimer<sup>27; 29</sup>. Furthermore, we expressed the Ig-V set domain (residues 27-159 or 26-159) of CD160 in *E. coli* as inclusion bodies and refolded the

proteins *in vitro*. The gel filtration chromatography again showed that CD160 eluted in the monomer fraction (15 kDa) (**Supplemental Figure 2**). We next determined the number of free thiol groups in the refolded CD160 using 5,5'-dithiobis 2-nitrobenzoate (DNTB), and one non-paired thiol group was detected (**Supplemental Figure 3**). Collectively, these results indicate that the extracellular domain of CD160 exists mainly in the monomeric form, consistent with the recent study using the baculovirus-expressed CD160 protein<sup>13</sup>.

*Binding affinity of CD160 toward HVEM.*

To analyze the binding properties of CD160 and HVEM, affinity measurements were performed using SPR. The extracellular domain of CD160 (I27-S159, 15 kDa) and the CRD1-3 (L1-Y103, 11 kDa) of HVEM with a biotin tag were expressed in *E. coli* and purified as described in the Materials and Methods. Although HVEM has at least eight disulfide bonds in its extracellular region, it was successfully refolded from inclusion bodies expressed in *E. coli*. The extracellular domain of CD160 was injected over sensor surfaces bearing biotinylated HVEM or biotinylated BSA (negative control). The affinity of CD160 to HVEM was measured by an equilibrium binding analysis. A range of CD160 concentrations were injected through the flow cells containing the immobilized HVEM (**Supplemental Figure 4A**).

The equilibrium binding curve for the binding of CD160 to HVEM is shown in **Figure 2A**. Consistent with the report by Stiles et al.<sup>13</sup>, our results show that CD160 binds directly to HVEM with a  $K_d$  of 0.34  $\mu$ M (**Table 1**), which is within the affinity range typical of cell surface receptors (**Supplemental Table 1**). This result strongly suggests that the monomeric form of CD160 is the predominant physiological species. We also performed a kinetic analysis of this interaction. The binding curves shown in **Figure 2B** fit well to a 1:1 Langmuir binding model. Although the  $K_d$  of the CD160-HVEM binding is comparable with that of the BTLA-HVEM binding, the CD160 binding displayed 2-fold slower kinetics than did BTLA (**Table 1 and**

**Figure 2C, and Supplemental Table 1).** CD160 may have a more inhibitory signaling function than BTLA because CD160 has a slower dissociation constant (**Supplemental Table 1**).

*The effect of HVEM on the binding of CD160 to the antiangiogenic anti-CD160 antibody CL1-R2.*

CL1-R2, a commercially available (MBL) anti-CD160 antibody, has been used in many studies; however, its binding characteristics toward CD160 are unknown. Therefore, we performed an SPR binding study between CD160 and the anti-CD160 antibody CL1-R2. The antibody was immobilized on a CM5 sensor chip by direct amine coupling. CD160 was injected over the sensor chip and exhibited strong binding to the anti-CD160 antibody (**Figure 3**). We next injected HVEM over the same chip to examine the effect of HVEM on the binding of CD160 to the anti-CD160 antibody (**Figure 3**). The response did not change during the HVEM injection, indicating that the anti-CD160 antibody CL1-R2 blocks CD160 binding to HVEM.

*CD160 competes with BTLA for binding to HVEM.*

BTLA is another coinhibitory molecule that interacts with HVEM. Although a cellular-based binding study showed that the CRD1 of HVEM was essential for both CD160 and BTLA binding and suggested that their binding sites potentially overlap <sup>7</sup>, it was not clear from the results of this study whether their binding sites actually overlapped or whether the molecules interfered with each other when binding to HVEM. Therefore, we performed a competition assay of CD160 and BTLA binding to HVEM using SPR.

We first expressed the extracellular domain of BTLA (residues S33-D135, 12 kDa) in *E. coli* as inclusion bodies, refolded the protein *in vitro* (**Supplemental Figure 5**), and performed an analysis of the binding of BTLA to HVEM (**Supplemental Figure 4B**). BTLA alone binds to HVEM with a  $K_d$  of 0.29  $\mu$ M (**Figure 4A, Table 1**), which is similar to the affinities of the murine BTLAs (0.42 and 0.97  $\mu$ M) obtained by an SPR analysis <sup>30</sup>. We next examined the

binding response when increasing concentrations of BTLA were injected over the HVEM with (squares) or without (triangles) an almost saturating concentration (1.5  $\mu$ M) of CD160 (**Figure 4B**). The difference between the responses in the presence or absence of CD160 (crosses) decreased as the concentration of BTLA increased, indicating that the binding was not additive and that BTLA showed typical competitive inhibition with CD160 for binding to HVEM <sup>31</sup>. These results suggest that the CD160 and BTLA binding sites on HVEM overlap or are close enough to each other that the binding of one molecule to HVEM blocks the binding of the other molecule.

To investigate the detailed features of the interactions of CD160 and BTLA with HVEM, two different-length HVEMs with biotin tags, (1) L1-H162: CRD1-4, and (2) L1-Y103: CRD1-3, were prepared using HEK293S GnTI<sup>-</sup> cells. The HVEMs were enzymatically biotinylated and immobilized on a streptavidin-coupled CM5 chip for the SPR analysis. Next, we tested whether recombinant HVEMs, refolded from inclusion bodies and produced in mammalian cells, exhibit any differences in their receptor binding. CD160 and BTLA exhibited almost the same affinities toward HVEM(L1-Y103) expressed in HEK293S GnTI<sup>-</sup> cells, indicating that the sugar modifications on HVEM do not contribute to the binding (**Table 2**). We used HVEM expressed in HEK293S GnTI<sup>-</sup> cells, designated as HVEMh, for the following assays.

To investigate the details of the CD160 binding site on HVEM, a longer version of HVEMh (L1-H162) was prepared. It exhibited a slightly lower but still similar binding affinity to the receptors, indicating that the CRD4 of HVEM does not play a significant role in CD160 and BTLA binding (**Table 2**). We then produced a series of HVEMh mutants (P17A, Y23A, V36A) because the mutated sites in CRD1 are known to be crucial for BTLA affinity, as identified by mutagenesis <sup>23</sup>(**Figure 4C, 4D, 4E**). A previous cellular-level binding report showed that the Y23A mutation reduced CD160 binding <sup>32</sup>. We performed affinity measurements of CD160 and

BTLA to these HVEMh mutants (**Figure 4C, 4D**). Although the P17A and V36A HVEMh mutants displayed 6-fold and 60- to 70-fold decreases in affinity for both CD160 and BTLA, respectively, the Y23A mutation resulted in a 20-fold reduction in the affinity for BTLA and completely abolished the affinity for CD160 even at concentrations exceeding 30  $\mu$ M (**Figure 4C, Table 2**). These results indicate that the Y23 residue of HVEM is more critical for CD160 binding than for BTLA binding; in contrast, the other mutations (P17A and V36A) have similar effects on the binding of HVEM to both CD160 and BTLA. Interestingly, the Y23A mutation of HVEMh also abolished the binding of HVEMh to HSV gD<sup>13</sup>, similar to the results for CD160. The crystal structures of the gD-<sup>33</sup> and BTLA-HVEM<sup>23</sup> complexes demonstrate that Y23 of HVEM penetrates deeply into HSV gD but that this residue simply attaches to the peripheral surface of BTLA (**Figure 4E**). These results suggest that the CD160-HVEM binding mode is similar to that of gD, but it is somewhat distinct from that of BTLA.

*LIGHT does not affect the binding of CD160 and BTLA to HVEM.*

Like other TNF-related ligands, LIGHT forms a homotrimer and potentially interacts with three HVEM molecules. In accordance with previous reports<sup>13</sup>, LIGHT binding to immobilized HVEMh exhibits an extremely high affinity with an avidity effect, quite unlike the binding to CD160 and BTLA (**Figure 5A**).

We next examined the effect of LIGHT on the HVEMh binding of CD160 and BTLA (**Figure 5B**). The binding responses observed for CD160 and BTLA to HVEMh were the same before and after the HVEM was saturated with LIGHT (**Figure 5B**). Furthermore, the HVEMh mutants (P17A, Y23A, V36A) (data not shown) displayed essentially the same affinity to LIGHT, indicating that the LIGHT binding site on HVEM does not overlap with either the CD160 or BTLA binding sites, consistent with the previous cellular-based studies<sup>23; 34</sup>.

*Functional Implications.*

A previous study showed that CD160 and BTLA do not colocalize on the same cell surface <sup>7</sup>, suggesting that these two coinhibitory molecules function in different compartments and do not associate before their interactions with HVEM. GPI-anchored CD160 probably exists in the lipid raft where the main signaling complexes, including the TCR/CD3 complexes, are normally localized and, thus, may have a more direct inhibitory effect on TCR/CD3 signaling. A transmembrane form of an alternative splice variant of CD160, possessing a putative phosphorylation site in its cytoplasmic region, was recently reported <sup>35</sup>. Alternatively, because BTLA is widely dispersed on the cell surface, we propose that CD160 and BTLA exert their inhibitory activities in different cell surface areas.

The present study has provided clear evidence that human CD160 is a monomeric receptor. CD160 and BTLA have similar affinities, but somewhat distinct kinetic parameters, for binding to HVEM. The slower dissociation of CD160 from HVEM suggests that CD160 may have the potential to induce dominant inhibitory signaling. Our competition assay showed that CD160 and BTLA cannot bind to HVEM simultaneously. Moreover, the mutagenesis study revealed that HVEM recognition by CD160 and BTLA seems to be similar, but some differences exist. Whether the potential dominant inhibitory function of CD160 is based on the slower dissociation of HVEM binding relative to that of BTLA will be addressed in future studies, specifically an *in vivo* study using CD160 knockout mice, which are not currently available. Furthermore, the CD160 expression on T cells and NK cells in the human immune system is significantly induced upon activation <sup>6; 7</sup>. These results strongly suggest that CD160 has an inhibitory function similar to that of another coinhibitory molecule, CTLA4, to prevent overactivation and terminate unnecessary immune responses. Therefore, the elucidation of the precise functional characteristics of the CD160-HVEM binding will be quite important for understanding its regulation, using either the soluble CD160 protein or an anti-CD160 antibody,

for future medical treatment of immune disorders, such as autoimmune diseases. Notably, a recent report<sup>28</sup> clearly demonstrated that the administration of the CD160 antibody, CL1-R2, in animal disease models significantly improved palliation, suggesting that CL1-R2 can be used in the medical treatment of ocular and tumor neoangiogenesis. HVEM can function not only as a ligand for its receptors including CD160 but also as a stimulatory receptor, resulting in a bidirectional signaling system. HVEM activates NF- $\kappa$ B to produce proinflammatory signals by binding to its receptors (ligands). Our present study demonstrates that the CL1-R2 antibody competes with HVEM for binding to CD160, introducing the possibility that HVEM-mediated cellular activation could be reduced by the CL1-R2 antibody. Further studies to investigate the molecular mechanism induced by the CL1-R2 antibody will be quite important for future medical applications.

## **MATERIALS AND METHODS**

*Production of the entire extracellular region of CD160 in HEK293S GnTI cells and N-terminal amino acid sequence analysis-* The DNA encoding the Ig-V domain (residues C26-S159) of CD160 was amplified from pGMCD160 (see the following section) by using 5'-GTA CCG GTT GCA TTA ACA TCA CCA GCT C -3' as the forward primer and 5'-CTG GTA CCT GAG AGA GTG CCT TCA TTA TGG C -3' as the reverse primer (designated RP1). The resultant fragments were digested with the restriction enzymes *AgeI* and *KpnI* and were ligated into the pHLsec vector (designated pHLCD160)<sup>36</sup>. For the expression of the entire extracellular region of CD160 (M1-S159), we extended the N-terminal region of CD160 by PCR using 5'-TGT GCC CTG GCC ATC CTG CTG GCA ATT GTG GAC ATC CAG TCT GGT GGA TGC ATT AAC ATC ACC AGC TC -3' as the forward primer and RP1 as the reverse primer, with pHLCD160 as the template. The resultant fragments were amplified using 5'-CGG AAT TCG

CCA CCA TGC TGT TGG AAC CCG GCA GAG GCT GCT GTG CCC TGG CCA TC -3' as the forward primer and RP1 as the reverse primer and were ligated into the *EcoRI/KpnI*-digested pHLsec vector. The final construct included CD160 (M1-S159) with the original signal sequence and the 6xHistidine-tag in tandem. The plasmid was transiently transfected by adding polyethyleneimine into 90% confluent HEK293S cells lacking *N*-acetylglucosaminyltransferase I (GnTI) activity or 293T cells<sup>36,37</sup>. The cells were cultured in DMEM (SIGMA) supplemented with 10% FCS (HyClone), L-glutamine, and nonessential amino acids (GIBCO). During transfection, the medium was changed to OPTI-MEM (GIBCO). The supernatant containing the His-tagged CD160 was collected 4 days after transfection and was purified by Ni-affinity chromatography and gel filtration with a Superdex 75 10/300 column (GE Healthcare). The purified extracellular region of CD160 was then digested with PNGase F (NEB) for 8 hours and analyzed by N-terminal amino acid sequencing (Shimadzu Biotech).

*Expression and refolding of the CD160 Ig-V domain, the BTLA Ig-V domain and LIGHT in Escherichia coli*- The DNA encoding the Ig-V domain (residues I27-S159) of CD160 was amplified from a human peripheral blood mononuclear cell cDNA library using 5'-GGA GAT ATA CAT ATG ATT AAC ATC ACC AGC TCA GC -3' as the forward primer and 5'-TAG GCA AGC TTA ACT GAG AGT GCC TTC ATT ATG GCT G -3' as the reverse primer. The resultant fragments were digested with the restriction enzymes *NdeI* and *HindIII* and were ligated into the pGMT7 vector (1) (designated pGMCD160). *Escherichia coli* strain BL21(DE3)pLysS cells (Novagen) harboring pGMCD160 produced CD160 within inclusion bodies. The inclusion bodies were isolated from the cell pellet by sonication and washed repeatedly with a wash solution containing 0.5% Triton X-100. The purified CD160 inclusion bodies were solubilized in a denaturant solution containing 6 M guanidine hydrochloride. The solubilized protein solution was diluted slowly in refolding buffer (0.1 M Tris-HCl, pH 8.0, 0.6 M L-arginine, 2

mM EDTA, 3.73 mM cystamine, 6.73 mM cysteamine) to a final protein concentration of 1-2  $\mu$ M and was stirred for 48 h at 4°C. The refolded mixture of CD160 was then concentrated with a VIVA FLOW50 system (Sartorius). CD160 was purified by gel filtration on a Superdex 75 column (GE Healthcare). The DNA encoding the Ig-V set domain (S33-D135) of BTLA was amplified from the cDNA (Accession No: BC107092, Open Biosystems) using 5'-GGA GAT ATA CAT ATG TCA TGT GAT GTA CAG CTT TAT ATA AAG AGA -3' as the forward primer and 5'-G GAA TTC TCA ATC TGT CAC ATA AAG AGT TGT TGA GTG -3' as the reverse primer. The resultant fragments were ligated into the pGMT7 vector. Inclusion bodies containing BTLA were obtained and purified according to the method described above. The DNA encoding the extracellular region of LIGHT (N93-V240) was amplified from the cDNA (Accession No: BC018058, Open Biosystems) using 5'-GGA GAT ATA CAT ATG AAC CCA GCA GCG CAT CTC -3' as the forward primer and 5'-CCC AAG CTT TCA CAC CAT GAA AGC CCC C -3' as the reverse primer. The resultant fragments were ligated into the pGMT7 vector, and three mutations derived from the cDNA were corrected by the QuikChange method. Inclusion bodies containing LIGHT were obtained and purified according to the method described above.

*Expression, refolding and biotinylation of HVEM (L1-Y103) in Escherichia coli-* The DNA encoding the CRD1-3 (L1-Y103) of HVEM was amplified from spleen cDNA (PCR Ready cDNA Human Spleen, PC40016, MBI) using 5' -GGA GAT ATA CAT ATG CTG CCG TCC TGC AAG GAG G -3' as the forward primer and 5'-CGC GGA TCC GTA AGC GCG GCA CGC G -3' as the reverse primer. The resultant fragments were digested with the restriction enzymes *NdeI* and *BamHI* and were ligated into the pGMT7 vector (designated pGMHVEM). The construct consisted of HVEM(L1-Y103) and the biotin tag in tandem. The pGMHVEM vector was transformed into BL21(DE3)pLysS cells, and inclusion bodies containing

HVEM(L1-Y103) with the biotin tag were obtained and purified by the method described above. The purified HVEM (L1-Y103) was biotinylated with Biotin Protein Ligase (BirA, Avidity) and subjected to gel filtration in HBS-EP buffer (10 mM Hepes, pH 7.4, 150 mM NaCl, 3 mM EDTA, 0.005% Surfactant P20) for the Surface Plasmon Resonance (SPR) analysis.

*Production and biotinylation of HVEMs in HEK293S GnTI cells-* The DNA encoding the CRD1-3 (L1-Y103) of HVEM was amplified from pGMHVEM using 5' -GT ACC GGT CTG CCG TCC TGC AAG GAG G -3' as the forward primer (designated FP1) and 5' - CCG CTC GAG TCA TTA ACG ATG ATT CCA CAC CAT TTT CTG -3' as the reverse primer. We also amplified CRD1-4 (L1-H162) of HVEM from spleen cDNA using FP1 as the forward primer and 5' - CCG CTC GAG TTA ACG ATG ATT CCA CAC CAT TTT CTG TGC ATC CAG AAT ATG ATG CAG GGT ACC GTG GGA GCT GCT GGT CCC-3' as the reverse primer. The resultant fragments were ligated into the pHLsec vector using the *AgeI* and *XhoI* restriction enzyme sites<sup>36</sup>. The final constructs consisted of the signal sequence ( $\beta$ -actin), HVEM(CRD1-3) or HVEM (CRD1-4), and the biotin tag in tandem. The plasmids were transiently transfected into HEK293S GnTI cells, and the supernatants containing the biotin-tagged HVEMs were biotinylated with Biotin Protein Ligase. The biotinylated HVEM was then dialyzed in HBS-EP buffer and used for the Surface Plasmon Resonance (SPR) analysis.

*Surface Plasmon Resonance (SPR) analysis-* SPR experiments were performed with a BIAcore3000 instrument (GE Healthcare). The biotinylated form of either HVEM or BSA (negative control) was immobilized on a research-grade CM5 chip (GE Healthcare), onto which streptavidin was covalently coupled. After exchanging the buffer to HBS-EP, the HVEM receptors (CD160, BTLA, and LIGHT) were injected over the immobilized HVEM. The binding response at each concentration was calculated by subtracting the equilibrium response

measured in the control flow cell from that in the HVEM flow cell. Kinetic constants were determined using the curve-fitting facility of the BIAEVALUATION 4.0 program (GE Healthcare) to fit the rate equations derived from the simple 1:1 Langmuir binding model ( $A + B \rightleftharpoons AB$ ). Additional curve fitting was performed with the ORIGIN 7 program (Microcal Software, Northampton, MA). Affinity constants ( $K_d$ ) were derived by fits to a single site-saturation model of the nonlinear curve fitting of the standard Langmuir binding isotherm. In the competitive binding experiment, BTLA preparations with or without CD160 (1.5  $\mu$ M), which was almost saturated, were passed over the immobilized HVEM. For the binding assay of CD160 toward the anti-CD160 antibody, CL1-R2 (MBL), the anti-CD160 antibody or the anti-CD161 antibody (negative control) was immobilized directly on a CM5 chip by amine coupling. CD160 and HVEM were injected over the immobilized anti-CD160 antibody.

## ACKNOWLEDGMENTS

We thank M. Kimura, T. Nakashima, and Y. Okabe for supporting this work. R.K. was supported by the Japan Society for the Promotion of Science (JSPS) Research Fellowship for Young Scientists. This work was partially supported by grants from the Ministry of Education, Culture, Sports, Science and Technology and the Ministry of Health, Labour and Welfare of Japan.

## REFERENCES

1. Arase, H. & Lanier, L. L. (2004). Specific recognition of virus-infected cells by paired NK receptors. *Rev Med Virol***14**, 83-93.
2. Bretscher, P. A. (1999). A two-step, two-signal model for the primary activation of precursor helper T cells. *Proc Natl Acad Sci U S A***96**, 185-90.
3. Gimmi, C. D., Freeman, G. J., Gribben, J. G., Gray, G. & Nadler, L. M. (1993). Human T-cell clonal anergy is induced by antigen presentation in the absence of B7 costimulation. *Proc Natl*

- Acad Sci U S A* **90**, 6586-90.
4. Freeman, G J., Wherry, E. J., Ahmed, R. & Sharpe, A. H. (2006). Reinvigorating exhausted HIV-specific T cells via PD-1-PD-1 ligand blockade. *J Exp Med* **203**, 2223-7.
  5. Greenwald, R. J., Freeman, G J. & Sharpe, A. H. (2005). The B7 family revisited. *Annu Rev Immunol* **23**, 515-48.
  6. Cai, G & Freeman, G J. (2009). The CD160, BTLA, LIGHT/HVEM pathway: a bidirectional switch regulating T-cell activation. *Immunol Rev* **229**, 244-58.
  7. Cai, G, Anumanthan, A., Brown, J. A., Greenfield, E. A., Zhu, B. & Freeman, G J. (2008). CD160 inhibits activation of human CD4<sup>+</sup> T cells through interaction with herpesvirus entry mediator. *Nat Immunol* **9**, 176-85.
  8. Agrawal, S., Marquet, J., Freeman, G J., Tawab, A., Bouteiller, P. L., Roth, P., Bolton, W., Ogg, G., Boumsell, L. & Bensussan, A. (1999). Cutting edge: MHC class I triggering by a novel cell surface ligand costimulates proliferation of activated human T cells. *J Immunol* **162**, 1223-6.
  9. Barakonyi, A., Rabot, M., Marie-Cardine, A., Aguerre-Girr, M., Polgar, B., Schiavon, V., Bensussan, A. & Le Bouteiller, P. (2004). Cutting edge: engagement of CD160 by its HLA-C physiological ligand triggers a unique cytokine profile secretion in the cytotoxic peripheral blood NK cell subset. *J Immunol* **173**, 5349-54.
  10. Le Bouteiller, P., Barakonyi, A., Giustiniani, J., Lenfant, F., Marie-Cardine, A., Aguerre-Girr, M., Rabot, M., Hilgert, I., Mami-Chouaib, F., Tabiasco, J., Boumsell, L. & Bensussan, A. (2002). Engagement of CD160 receptor by HLA-C is a triggering mechanism used by circulating natural killer (NK) cells to mediate cytotoxicity. *Proc Natl Acad Sci U S A* **99**, 16963-8.
  11. Li, Q., Smith, A. J., Schacker, T. W., Carlis, J. V., Duan, L., Reilly, C. S. & Haase, A. T. (2009). Microarray analysis of lymphatic tissue reveals stage-specific, gene expression signatures in HIV-1 infection. *J Immunol* **183**, 1975-82.
  12. Blackburn, S. D., Shin, H., Haining, W. N., Zou, T., Workman, C. J., Polley, A., Betts, M. R., Freeman, G J., Vignali, D. A. & Wherry, E. J. (2009). Coregulation of CD8<sup>+</sup> T cell exhaustion by multiple inhibitory receptors during chronic viral infection. *Nat Immunol* **10**, 29-37.
  13. Stiles, K. M., Whitbeck, J. C., Lou, H., Cohen, G. H., Eisenberg, R. J. & Krummenacher, C. (2010). Herpes simplex virus glycoprotein D interferes with binding of herpesvirus entry mediator to its ligands through downregulation and direct competition. *J Virol* **84**, 11646-60.
  14. Harrop, J. A., McDonnell, P. C., Brigham-Burke, M., Lyn, S. D., Minton, J., Tan, K. B., Dede, K., Spanpanato, J., Silverman, C., Hensley, P., DiPrinzio, R., Emery, J. G., Deen, K., Eichman, C., Chabot-Fletcher, M., Truneh, A. & Young, P. R. (1998). Herpesvirus entry mediator ligand (HVEM-L), a novel ligand for HVEM/TR2, stimulates proliferation of T cells and inhibits HT29 cell growth. *J Biol Chem* **273**, 27548-56.
  15. Steinberg, M. W., Shui, J. W., Ware, C. F. & Kronenberg, M. (2009). Regulating the mucosal

- immune system: the contrasting roles of LIGHT, HVEM, and their various partners. *Semin Immunopathol***31**, 207-21.
16. Tamada, K., Shimozaki, K., Chapoval, A. I., Zhai, Y., Su, J., Chen, S. F., Hsieh, S. L., Nagata, S., Ni, J. & Chen, L. (2000). LIGHT, a TNF-like molecule, costimulates T cell proliferation and is required for dendritic cell-mediated allogeneic T cell response. *J Immunol***164**, 4105-10.
  17. Tamada, K., Shimozaki, K., Chapoval, A. I., Zhu, G., Sica, G., Flies, D., Boone, T., Hsu, H., Fu, Y. X., Nagata, S., Ni, J. & Chen, L. (2000). Modulation of T-cell-mediated immunity in tumor and graft-versus-host disease models through the LIGHT co-stimulatory pathway. *Nat Med***6**, 283-9.
  18. Yu, P., Lee, Y., Liu, W., Chin, R. K., Wang, J., Wang, Y., Schietinger, A., Philip, M., Schreiber, H. & Fu, Y. X. (2004). Priming of naive T cells inside tumors leads to eradication of established tumors. *Nat Immunol***5**, 141-9.
  19. Granger, S. W. & Rickert, S. (2003). LIGHT-HVEM signaling and the regulation of T cell-mediated immunity. *Cytokine Growth Factor Rev***14**, 289-96.
  20. Harrop, J. A., Reddy, M., Dede, K., Brigham-Burke, M., Lyn, S., Tan, K. B., Silverman, C., Eichman, C., DiPrinzio, R., Spampanato, J., Porter, T., Holmes, S., Young, P. R. & Truneh, A. (1998). Antibodies to TR2 (herpesvirus entry mediator), a new member of the TNF receptor superfamily, block T cell proliferation, expression of activation markers, and production of cytokines. *J Immunol***161**, 1786-94.
  21. Shaikh, R. B., Santee, S., Granger, S. W., Butrovich, K., Cheung, T., Kronenberg, M., Cheroutre, H. & Ware, C. F. (2001). Constitutive expression of LIGHT on T cells leads to lymphocyte activation, inflammation, and tissue destruction. *J Immunol***167**, 6330-7.
  22. Wang, Y., Subudhi, S. K., Anders, R. A., Lo, J., Sun, Y., Blink, S., Wang, Y., Wang, J., Liu, X., Mink, K., Degrandi, D., Pfeffer, K. & Fu, Y. X. (2005). The role of herpesvirus entry mediator as a negative regulator of T cell-mediated responses. *J Clin Invest***115**, 711-7.
  23. Compaan, D. M., Gonzalez, L. C., Tom, I., Loyet, K. M., Eaton, D. & Hymowitz, S. G. (2005). Attenuating lymphocyte activity: the crystal structure of the BTLA-HVEM complex. *J Biol Chem***280**, 39553-61.
  24. Han, P., Goularte, O. D., Rufner, K., Wilkinson, B. & Kaye, J. (2004). An inhibitory Ig superfamily protein expressed by lymphocytes and APCs is also an early marker of thymocyte positive selection. *J Immunol***172**, 5931-9.
  25. Watanabe, N., Gavrieli, M., Sedy, J. R., Yang, J., Fallarino, F., Loftin, S. K., Hurchla, M. A., Zimmerman, N., Sim, J., Zang, X., Murphy, T. L., Russell, J. H., Allison, J. P. & Murphy, K. M. (2003). BTLA is a lymphocyte inhibitory receptor with similarities to CTLA-4 and PD-1. *Nat Immunol***4**, 670-9.
  26. Deppong, C., Juehne, T. I., Hurchla, M., Friend, L. D., Shah, D. D., Rose, C. M., Bricker, T. L.,

- Shornick, L. P., Crouch, E. C., Murphy, T. L., Holtzman, M. J., Murphy, K. M. & Green, J. M. (2006). Cutting edge: B and T lymphocyte attenuator and programmed death receptor-1 inhibitory receptors are required for termination of acute allergic airway inflammation. *J Immunol***176**, 3909-13.
27. Anumanthan, A., Bensussan, A., Boumsell, L., Christ, A. D., Blumberg, R. S., Voss, S. D., Patel, A. T., Robertson, M. J., Nadler, L. M. & Freeman, G. J. (1998). Cloning of BY55, a novel Ig superfamily member expressed on NK cells, CTL, and intestinal intraepithelial lymphocytes. *J Immunol***161**, 2780-90.
28. Chabot, S., Jabrane-Ferrat, N., Bigot, K., Tabiasco, J., Provost, A., Golzio, M., Noman, M. Z., Giustiniani, J., Bellard, E., Brayer, S., Aguerre-Girr, M., Meggetto, F., Giuriato, S., Malecaze, F., Galiacy, S., Jais, J. P., Chose, O., Kadouche, J., Chouaib, S., Teissie, J., Abitbol, M., Bensussan, A. & Le Bouteiller, P. (2011). A novel antiangiogenic and vascular normalization therapy targeted against human CD160 receptor. *J Exp Med***208**, 973-86.
29. Maiza, H., Leca, G., Mansur, I. G., Schiavon, V., Boumsell, L. & Bensussan, A. (1993). A novel 80-kD cell surface structure identifies human circulating lymphocytes with natural killer activity. *J Exp Med***178**, 1121-6.
30. Nelson, C. A., Fremont, M. D., Sedy, J. R., Norris, P. S., Ware, C. F., Murphy, K. M. & Fremont, D. H. (2008). Structural determinants of herpesvirus entry mediator recognition by murine B and T lymphocyte attenuator. *J Immunol***180**, 940-7.
31. Shiroishi, M., Tsumoto, K., Amano, K., Shirakihara, Y., Colonna, M., Braud, V. M., Allan, D. S., Makadzange, A., Rowland-Jones, S., Willcox, B., Jones, E. Y., van der Merwe, P. A., Kumagai, I. & Maenaka, K. (2003). Human inhibitory receptors Ig-like transcript 2 (ILT2) and ILT4 compete with CD8 for MHC class I binding and bind preferentially to HLA-G. *Proc Natl Acad Sci U S A***100**, 8856-61.
32. Cheung, T. C., Steinberg, M. W., Osborne, L. M., Macauley, M. G., Fukuyama, S., Sanjo, H., D'Souza, C., Norris, P. S., Pfeffer, K., Murphy, K. M., Kronenberg, M., Spear, P. G. & Ware, C. F. (2009). Unconventional ligand activation of herpesvirus entry mediator signals cell survival. *Proc Natl Acad Sci U S A***106**, 6244-9.
33. Carfi, A., Willis, S. H., Whitbeck, J. C., Krummenacher, C., Cohen, G. H., Eisenberg, R. J. & Wiley, D. C. (2001). Herpes simplex virus glycoprotein D bound to the human receptor HveA. *Mol Cell***8**, 169-79.
34. Sarrias, M. R., Whitbeck, J. C., Rooney, I., Ware, C. F., Eisenberg, R. J., Cohen, G. H. & Lambris, J. D. (2000). The three HveA receptor ligands, gD, LT-alpha and LIGHT bind to distinct sites on HveA. *Mol Immunol***37**, 665-73.
35. Giustiniani, J., Bensussan, A. & Marie-Cardine, A. (2009). Identification and characterization of a transmembrane isoform of CD160 (CD160-TM), a unique activating receptor selectively

- expressed upon human NK cell activation. *J Immunol***182**, 63-71.
36. Aricescu, A. R., Assenberg, R., Bill, R. M., Busso, D., Chang, V. T., Davis, S. J., Dubrovsky, A., Gustafsson, L., Hedfalk, K., Heinemann, U., Jones, I. M., Ksiazek, D., Lang, C., Maskos, K., Messerschmidt, A., Macieira, S., Peleg, Y., Perrakis, A., Poterszman, A., Schneider, G., Sixma, T. K., Sussman, J. L., Sutton, G., Tarboureich, N., Zeev-Ben-Mordehai, T. & Jones, E. Y. (2006). Eukaryotic expression: developments for structural proteomics. *Acta Crystallogr D Biol Crystallogr***62**, 1114-24.
37. Hashiguchi, T., Kajikawa, M., Maita, N., Takeda, M., Kuroki, K., Sasaki, K., Kohda, D., Yanagi, Y. & Maenaka, K. (2007). Crystal structure of measles virus hemagglutinin provides insight into effective vaccines. *Proc Natl Acad Sci U S A***104**, 19535-40.

## FIGURE LEGENDS

### **Figure 1. The extracellular Ig-V set domain of CD160h is monomeric.**

(A) Gel filtration chromatography (Superdex 75 10/300) purification of the CD160h Ig-V set domain (15 kDa) expressed in HEK293S GnTI cells. The HEK293S GnTI cell culture supernatant containing His-tagged CD160h was purified by Ni-NTA affinity chromatography. All of the eluted fractions containing CD160h were then subjected to gel filtration chromatography. The CD160h Ig-V set domain eluted at approximately 15 kDa (Arrowheads 4-6). Arrowheads 1-6 indicate the fraction numbers. Arrowhead 1 also indicates the void volume ( $V_0$ ) peak. The bars indicate the elution positions of the molecular mass markers.

(B) The CD160h Ig-V set domain purified in (A) was denatured with SDS sample buffer without reducing agents (e.g., DTT) and resolved on a 15% SDS-PAGE gel followed by western blotting with an anti-6xHis antibody. The numbers 1-6 on the top of the membrane are the fractions 1-6 shown in (A). M indicates the protein size marker. The monomeric CD160h Ig-V set domain ran as multiple bands due to different sugar modifications. We confirmed this conclusion by Endoglycosidase H (Endo H) or PNGase F digestion (data not shown). The asterisk (\*) indicates the CD160h Ig-V set domain before gel filtration chromatography purification (immediately after purification by Ni-NTA affinity chromatography).

(C) Amino-acid sequence of CD160 deduced from the cDNA sequence. The asterisk (\*) indicates the position of the predicted N-glycosylation site. The double asterisk (\*\*) indicates the position of the N-glycosylation site confirmed by an N-terminal sequence analysis. Cysteine residues within the Ig-V set domain are boxed.

### **Figure 2. CD160 binds to HVEM**

(A) Plots of the equilibrium binding responses of the extracellular Ig-V set domain of CD160 to

HVEM ( $K_d \sim 0.34 \mu\text{M}$ ). The purified, recombinant, C-terminally biotin-tagged HVEM was immobilized on a CM5 sensor chip, and different concentrations of purified CD160 were injected on the chip.

(B) Kinetic analysis of CD160 binding to HVEM. Low concentrations of purified CD160 (80, 40, 20, 10, 5, or 2.5 nM) were injected at a flow rate of 50  $\mu\text{l}/\text{min}$  on the same sensor chip used in (A) (solid lines). The rate equations derived from the 1:1 binding model were fitted to the association and dissociation phases of all injections (dotted lines).

(C) Kinetic analysis of BTLA binding to HVEM. Low concentrations of purified BTLA (40, 20, 10, 5, 2.5 nM) were injected at a flow rate of 50  $\mu\text{l}/\text{min}$  on the same sensor chip used in (A) (solid lines). Rate equations derived from the 1:1 binding model were fitted to the association and dissociation phases of all injections (dotted lines).

**Figure 3. The effect of HVEM on the binding of CD160 to anti-CD160 mAb.**

Anti-CD160 mAb (CL1-R2) was immobilized on a CM5 sensor chip by amine coupling and generated 3,000 RU. Solutions containing 6  $\mu\text{M}$  CD160 and 6  $\mu\text{M}$  HVEM were injected sequentially on the chip surface as indicated (arrowheads). For chip regeneration, glycine (pH2.0) was injected.

**Figure 4. The effect of BTLA on CD160 binding to HVEM.**

(A) Equilibrium binding analysis of BTLA against HVEM on the same sensor chip used in the experiment shown in Figure 2 ( $K_d \sim 0.29 \mu\text{M}$ ). The estimated saturation level of BTLA was calculated by nonlinear curve fitting [1,280 response units (RU)].

(B) Binding of BTLA alone (filled triangles) or mixed with CD160 (filled squares) on the same sensor chip used in the experiment shown in (A). The CD160 concentration was 1.5  $\mu\text{M}$  (Figure 2A, dotted line). The difference in the binding observed in the presence or absence of CD160 is

plotted (crosses).

(C) Equilibrium binding analysis of BTLA against wild type HVEMh and HVEMh point mutants (P17A, Y23A, V36A). BTLA bound to the HVEMh mutants P17A, Y23A, and V36A with  $K_d$  values of 17  $\mu$ M, 5.3  $\mu$ M, and 1.4  $\mu$ M, respectively.

(D) Equilibrium binding analysis of CD160 against wild-type HVEMh and HVEMh point mutants (P17A, Y23A, V36A). CD160 bound to the HVEMh mutants P17A and V36A with  $K_d$  values of 23 and 2.2  $\mu$ M, respectively. The Y23A mutant diminished the affinity for CD160 at concentrations exceeding 30  $\mu$ M.

(E) Crystal structures of the BTLA-HVEM (left)<sup>23</sup> and HSV gD-HVEM (right)<sup>33</sup> complexes. Surface representations of BTLA (green, left) and HSV gD (orange, right) are shown. A cartoon model of HVEM (cyan) showing the three residues, P17, Y23, and V36, where the mutations were introduced is also shown.

**Figure 5. The effect of LIGHT on the binding of CD160 and BTLA to HVEM.**

(A) Kinetic analysis of LIGHT binding to HVEM. C-terminal biotin-tagged HVEMh was coupled to a streptavidin-immobilized CM5 sensor chip and generated 500 RU. Different concentrations of purified LIGHT were injected at a flow rate of 50  $\mu$ l/min on the chip surface. The binding curves were fitted to a 1:1 Langmuir binding model, and the  $K_d$  value calculated by the  $k_{off}/k_{on}$  ratio was 30 nM.

(B) Binding of CD160 (solid line) and BTLA (dotted line) to HVEMh before and after the injection of LIGHT to a saturating level. Arrowheads with solid lines indicate the beginning of the CD160 and BTLA injections. The arrowhead with the dotted line indicates the beginning of the LIGHT injection. The sensor chip used was the same as that in (A).

**Table 1. Affinity constants of the interactions of CD160 and BTLA with refolded HVEM.**

Immobilized	Injected, $K_d$ at 25°C	
	CD160	BTLA
HVEM (L1-Y103)	$0.34 \pm 0.01 \mu\text{M}$ (4)	$0.29 \pm 0.01 \mu\text{M}$ (4)
	* $0.17 \mu\text{M}$ <sup>a</sup>	* $0.25 \mu\text{M}$

Values are presented as mean  $\pm$  standard deviation. The number of measurements is shown in parentheses. The immobilized level of HVEM is approximately 2,500 response units. The  $K_d$  values were obtained from the equilibrium analysis. \*Values were reported previously<sup>13</sup> and are shown here for comparison. <sup>a</sup> The  $K_d$  values were calculated by the simple 1:1 Langmuir binding model.

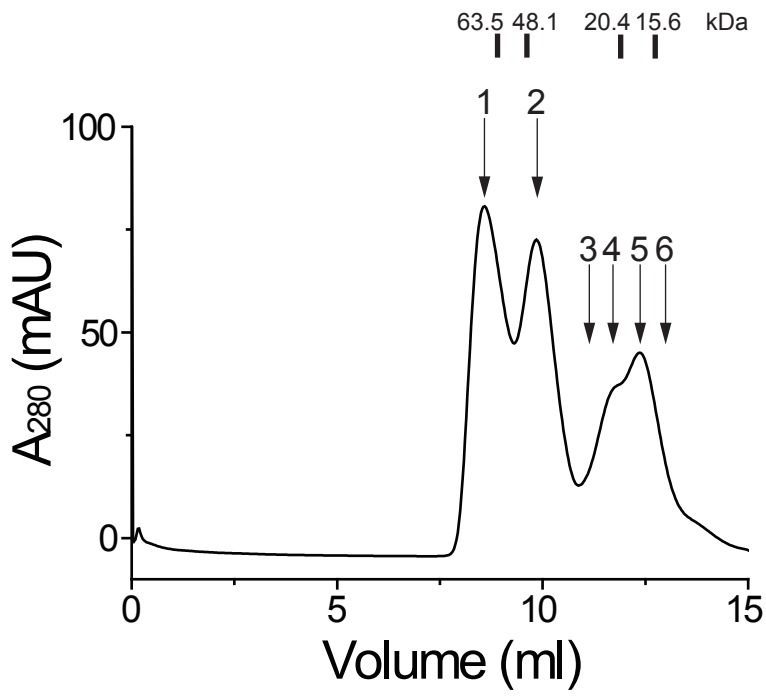
**Table 2. Summary of affinity constants for the interactions of CD160 and BTLA with HVEMs purified from HEK293S GNTI cells.**

Immobilized	Injected, $K_d$ at 25°C	
	CD160	BTLA
HVEMh (L1-H162)	$0.82 \pm 0.03 \mu\text{M}$ (2)	$0.48 \pm 0.10 \mu\text{M}$ (2)
HVEMh (L1-Y103)	$0.36 \pm 0.03 \mu\text{M}$ (4)	$0.22 \pm 0.04 \mu\text{M}$ (4)
HVEMh (L1-Y103) P17A	$23 \pm 0.26 \mu\text{M}$ (4)	$17 \pm 0.28 \mu\text{M}$ (4)
HVEMh (L1-Y103) Y23A	NB	$5.3 \pm 0.02 \mu\text{M}$ (4)
HVEMh (L1-Y103) V36A	$2.3 \pm 0.15 \mu\text{M}$ (4)	$1.4 \pm 0.32 \mu\text{M}$ (4)

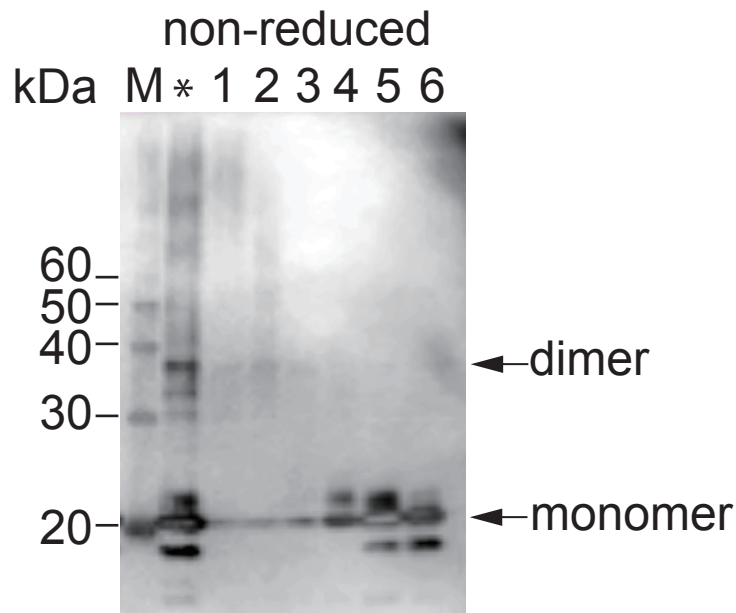
Values are presented as mean  $\pm$  standard deviation. The number of measurements is shown in parentheses. The immobilized levels of HVEMs ranged from 500 to 1,300 response units. NB, no binding was observed at a CD160 concentration of 30  $\mu\text{M}$ . The  $K_d$  values were obtained from the equilibrium analysis.

Figure 1

A



B



C

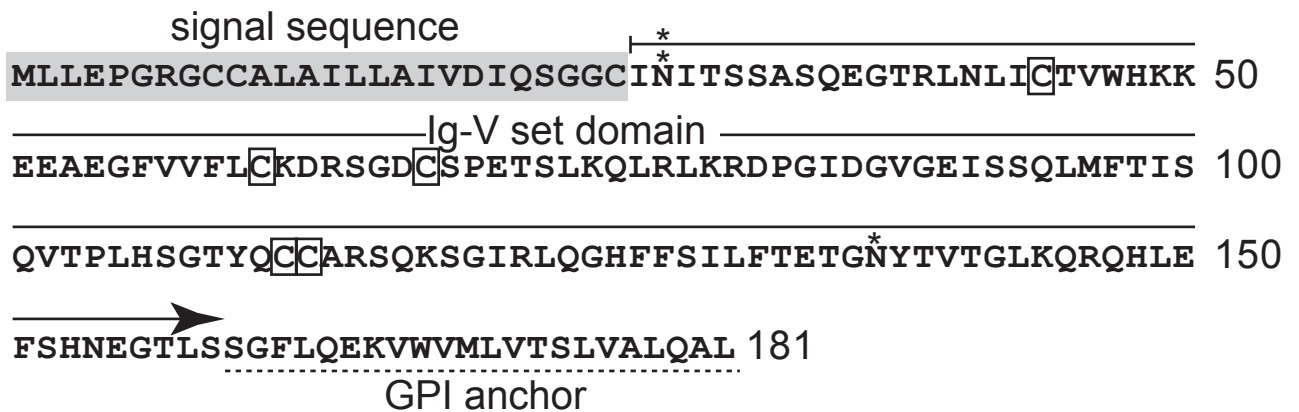


Figure 2

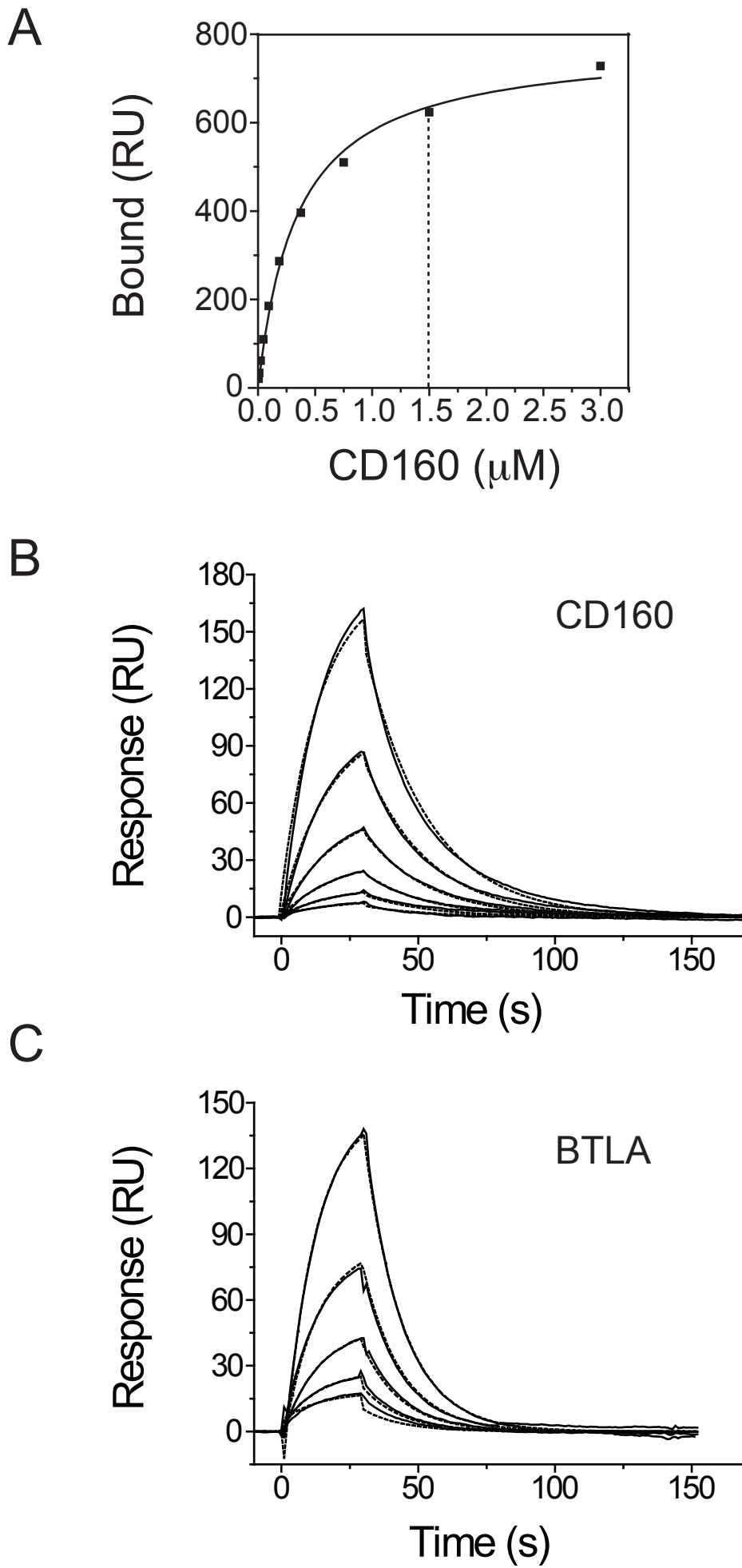


Figure 3

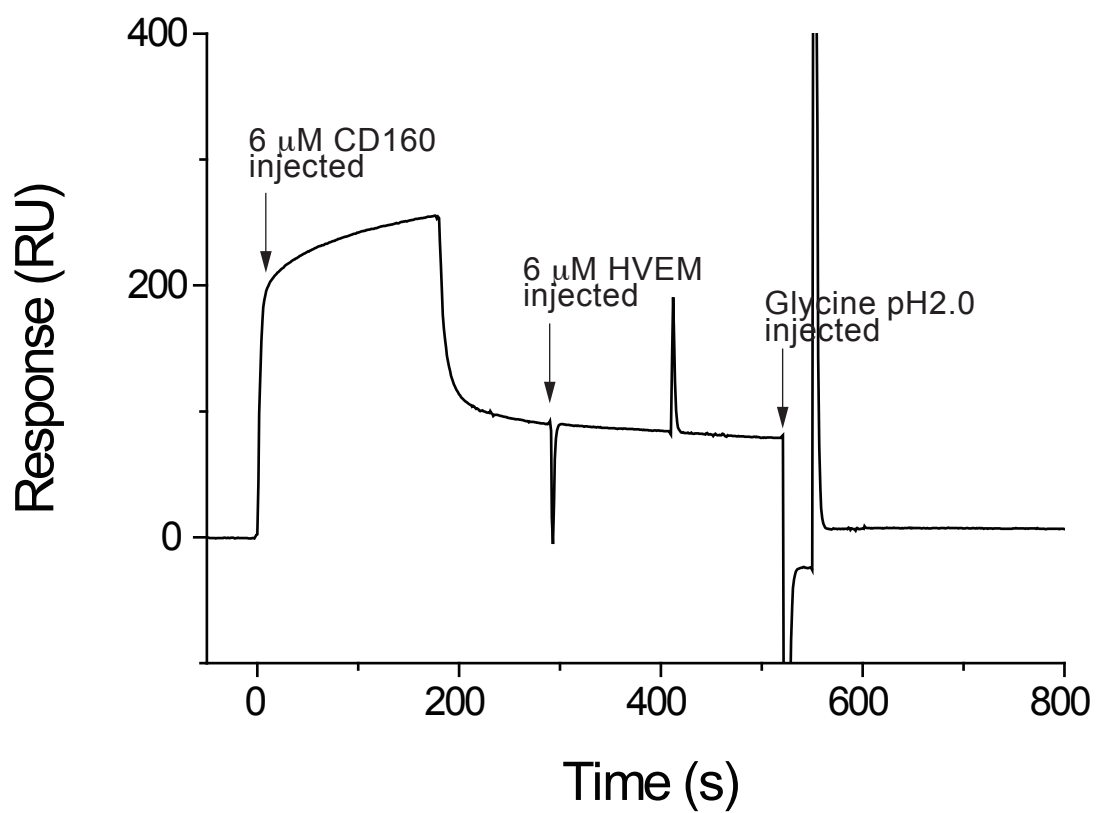


Figure 4

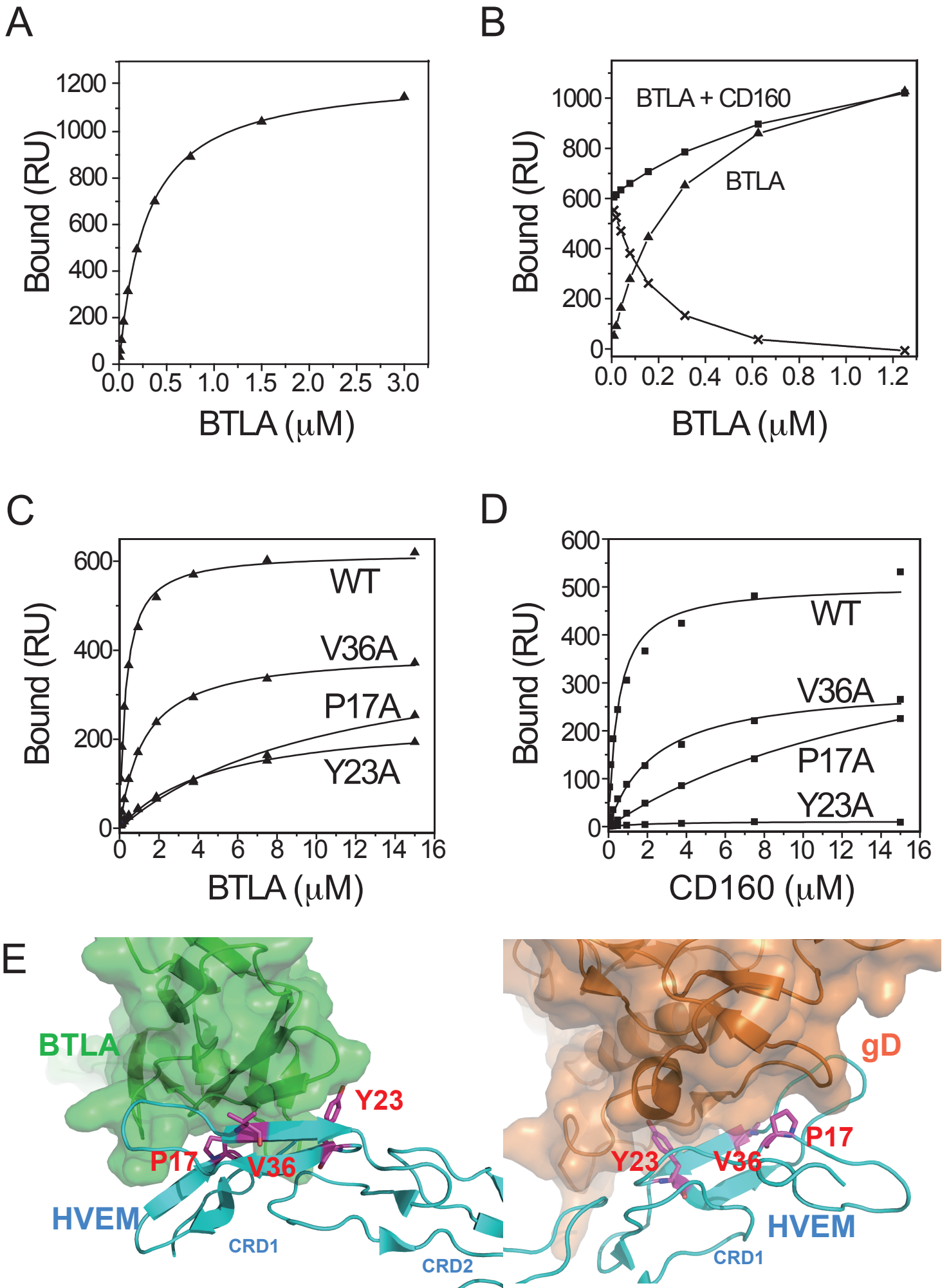


Figure 5

